Electronic structure of GaAs under strain

N. E. Christensen*
Max-Planck-Institut für Festkörperforschung, D-7000 Stuttgart 80, Federal Republic of Germany
(Received 9 July 1984)

Results of self-consistent relativistic band calculations for GaAs under hydrostatic as well as uniaxial strain are presented. Deformation potentials related to the splitting of the valence-band edge (Γ_{15}^{v}) are calculated with and without inclusion of spin-orbit coupling. The trigonal-shear deformation potentials that agree with experiments correspond to an internal-strain parameter $\zeta=0.6\pm0.1$. The calculated values, 16–19 eV, of the optical deformation potential d_0 are substantially smaller than the published experimental results ($\simeq$41 eV). The E_0 gap obtained in the local-density approximation is 0.25 eV. A method of correcting for this error and for calculating, self-consistently, the lowest s-like conduction band is described, and used to derive pressure dependences of the gaps and conduction-band masses. The parameters for this adjustment of the conduction band are determined for zero pressure, and can be kept pressure independent. We find $(1/m_c^*)dm_c^*/dP = 0.68\times10^{-2}$ kbar^{-1}. The pressure at which conduction-band inversion occurs is 30.5 kbar. The value calculated for shear deformation potential $\mathscr{E}_2^L$ is 19 eV for $\zeta=0.6$. The spin-orbit-induced splitting of the lowest conduction band for $\vec{k}\|[110]$ and the additional strain-induced splitting are calculated and related to experimental results for spin relaxation of photoexcited electrons.

I. INTRODUCTION

The electronic energy bands of gallium arsenide have been the subject of many theoretical and experimental works over the last two decades. The results of calculations using empirical nonlocal pseudopotentials obtained by Chelikowsky and Cohen[1] offer an interpretation of optical spectroscopic data. For details of the band structure, readers are referred to this paper[1] and the reviews, Refs. 2 and 3, and the references therein.

The majority of first-principles band calculations employ the local-density approximation for calculation of exchange-correlation effects. It is well known that this leads to gaps in insulators which are too small[4] when compared to experiments. The magnitude of this error is, however, in several cases, underestimated because relativistic shifts are neglected. The direct (p to s) band gap in GaAs is typically calculated (nonrelativistically) to be 1.1–1.2 eV, as opposed to the experimental value, 1.42 eV ($T=300$ K). As demonstrated[5] recently, relativistic shifts are important even in the relatively low-Z materials such as Ge and GaAs. The band gap in GaAs, which we calculate[5] including the relativistic effects, and relaxing the Ga $3d$ states, is 0.25 eV and Ge is, in the relativistic model, almost a metal. The calculations have further shown that this error does not simply appear as a uniform downshift of the conduction bands. The dispersion is also in error, and this error is enhanced by the relativistic effects since these are particularly large for the s-like conduction state at Γ. This also means that the calculated conduction-band masses,[6,7] particularly at Γ, are very much in error, $m_c^*\simeq0.012m_0$, i.e., less than one-fifth of the observed value,[3] $0.067m_0$. In the present work we wish to calculate the strain dependence of the band gaps and conduction-band masses in GaAs. Therefore a method has been introduced that corrects for the too small band-gap values obtained by the local-density scheme. This method is briefly discussed in Sec. II, where we present the calculated band structure, unadjusted as well as adjusted.

The equilibrium volume, bulk modulus, and hydrostatic deformation potentials are discussed in Sec. III. Furthermore, a relation between the direct band gap E_0 and the pressure P is given. Tetragonal- and trigonal-shear deformation potentials calculated with and without spin-orbit (SO) coupling are given in Sec. IV, together with shear dependences of the conduction-band masses.

II. LOCAL-DENSITY BANDS AND ADJUSTED BANDS

The band structure of gallium arsenide as calculated in the local-density approximation, using the Ceperley-Alder[8,9] description with relativistic corrections,[10] is shown in Fig. 1. We use the linear-muffin-tin-orbital (LMTO) method,[11] and introduce[12–14] "empty spheres." Used in this way, and including the so-called "combined correction term,"[11] the LMTO method yields very accurate[5] band structures, even for structures, like that of zinc-blende, which are open. The local-density band structure, Fig. 1, is discussed in detail elsewhere.[5] Here we only need to compare it to a few experimental results and to the empirical pseudopotential calculation by Chelikowsky and Cohen in order to establish where and how much it is in error. This comparison is made in Table I.

The LMTO self-consistent calculation used three energy panels, i.e., three sets of E_v values[11] were chosen. The lowest panel covers the Ga $3d$– and As $4s$–band regimes, whereas the second panel contains the rest of the occupied states. The conduction states were calculated using a separate panel together with the self-consistent potential generated from the two panels just mentioned. The Ga $3d$ bands (Fig. 1) appear almost dispersionless, but it was

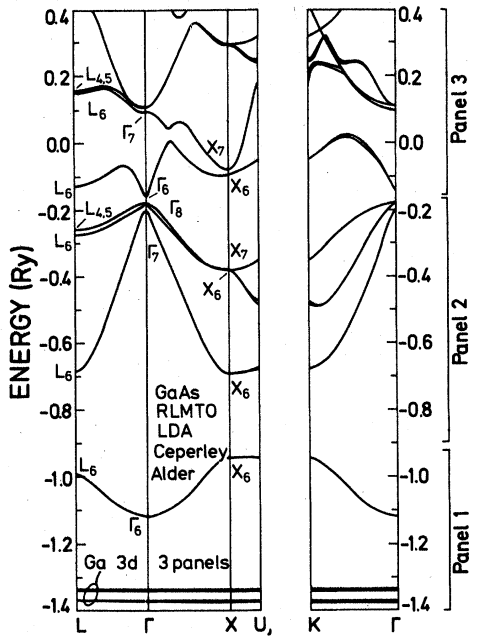

FIG. 1. Relativistic self-consistent local-density band structure of GaAs. Spin-orbit coupling is included. The lattice parameter corresponds to the experimental equilibrium volume. The range of the three energy panels (see text) are indicated. All atomic-sphere radii (Ga, As, and two "empty spheres") are chosen equal ($S=2.6303$ a.u.).

nevertheless found necessary to include them as band states. Treating the Ga $3d$ states as (renormalized) frozen-core states leads to a larger local-density (LD) band gap[5] ($E_0=0.56$ eV). A choice of atomic-sphere radii that would make the renormalization effects of the Ga $3d$ states negligible would require radii of the four spheres in the primitive cell so different in magnitude that errors due to spurious overlaps could not be excluded.

The valence bands obtained by the calculation (LD, Table I) agree well with experiments (concerning the spectral position of the Ga $3d$ bands, see Ref. 5). As mentioned earlier, the conduction bands, on the other hand, differ substantially from the data obtained from optical experiments. The present calculation shows[5] that previous LD theories omitting relativistic effects largely underestimate these errors. The gap which we find is only 0.25 eV, showing that the relativistic shifts of the s states relative to the p states are not negligible, even for the relatively low-Z materials such as Ga, As, and Ge. In fact, a relativistic, local-density calculation for Ge yields a gap which is less than 0.02 eV, i.e., Ge is almost metallic in this approximation. The Darwin shifts of the s states are positive, but they are smaller in magnitude than the (negative) mass-velocity shifts. This is the reason why the gaps calculated in the LD scheme with inclusion of relativity are so much smaller than those obtained from nonrelativistic calculations. This suggests an obvious way for introducing corrections to the band structure which yield s-

TABLE I. GaAs energy eigenvalues (eV).

Level	Empirical nonlocal pseudopotential[a]	LD Present work fully relativistic local density	LD+V_w Present work with extra potentials	Experiment
Γ_6^v	−12.55	−12.85		
Γ_7^v (Δ_0)	−0.35	−0.36	−0.343	−0.341
Γ_8^v	0.00	0.00	0.00	
Γ_6^c (E_0)	1.51	0.25	1.46	1.49
Γ_7^c	4.55	3.61	3.87	
Γ_8^c	4.71	3.81	4.08	
X_6^v	−9.83	−10.49		
X_6^v	−6.88	−7.06		
X_6^v	−2.99	−2.90		
X_7^v	−2.89	−2.83		
X_6^c	2.03	1.05	1.95	1.95
X_7^c	2.38	1.28	2.75	
L_6^v	−10.60	−11.20		
L_6^v	−6.83	−6.94		
L_6^v	−1.42	−1.39	−1.31	
$L_{4,5}^v$	−1.20	−1.18	−1.10	
L_6^c	1.82	0.67	1.82	1.81

[a] Reference 1.

like conduction bands in better agreement with experiment; we may try to introduce false "Darwin shifts." This is done in the present work by adding extra potentials which are sharply peaked (almost δ-function-like) on the atomic sites. Such localized, positive potentials act essentially only on s states, mainly on $1s$, and therefore produce upshifts of s states relative to the states of higher angular momenta.

The extra potentials, added to the local-density potential at all stages of the self-consistency iteration, were taken to be of the form

$$V_w(r)=V_0\frac{r_0}{r}e^{-(r/r_0)^2}. \tag{1}$$

A given shift can be produced by several different choices of V_0 and r_0, and the effect on the band structure is not critically dependent on which combination of the parameters has been chosen, as long as the range parameter r_0 is taken to be small. For Si, Ge, and GaAs we choose r_0 typically of the order of 0.015 a.u., and we adjust, by trial and error, V_0. For small values of r_0 the shift of the outer s states in an atom may be considered as propagation from the lowest-lying $1s$ states to the outer states as a consequence of orthogonality of the wave functions. This explains why details of $V_w(r)$ are not important; a given artificial $1s$ Darwin shift leads to a certain shift in, for example, the $4s$-$4p$ separation in Ge. This is illustrated in Fig. 2, where $\Delta\epsilon_{sp}$, the shift in the $4s$-$4p$ separation for Ge, Ga, and As, is plotted as a function of the $1s$ energy shift. In the case of Ge, preliminary estimates of V_0 and r_0 can be made from the atomic calculation alone. The direct gap at Γ (p to s) is 0.89 eV, i.e., we need to produce a $4s$-$4p$ energy shift of this order of magnitude. The atomic calculations show that this can be done by choosing $r_0\simeq0.015$ a.u. and $V_0\simeq320$ Ry. Fixing r_0 to 0.005 a.u. in the atomic as well as in the self-consistent LMTO calculation, we find that the conduction-band edges at X, L, and Γ vary with V_0 as shown in Fig. 3. It follows that the gap is indirect ($\Gamma\rightarrow L$), in agreement with experiment, but a value of V_0 that produces the correct gap at Γ leads to an L_c energy which is still far too low, ~0.4 eV, as opposed to the observed 0.76 eV. Thus, we cannot, using the procedure outlined above, obtain an s-like conduction band which has the correct energy at Γ and simultaneously the correct dispersion. In particular, as also follows from Fig. 3, the X_c level is far too little affected by the adjusting potentials $V_w(r)$ centered on the Ge sites. The reason for this is obvious when the probability-amplitude distributions[5] are calculated for the three states Γ_c, X_c, and L_c. The X_c state has almost no density on the Ge site—it is mainly located in the "interstitial" regime, that is, in our language, in the empty spheres. Γ_c, on the other hand, has almost no density in the empty spheres, whereas L_c represents an intermediate case. Similar observations were made by Rompa *et al.*[15] This means that, in order to also adjust the conduction bands at X and L, we must also add extra potentials in the empty spheres. The procedure for obtaining a suitable set of parameters for GaAs was then to make an estimate of parameters for the Ga and As extra potentials (they were chosen to be equal and identical to the Ge parameters referred to above), and then make the fine tuning of the conduction band by trial-and-error adjustment of the empty-sphere parameters. The bands of GaAs in the gap region are shown in Fig. 4, and eigenvalues for this adjusted band structure are listed in Table I. The density-of-states functions are shown in Fig. 5. It follows (Table I) that the adjusted bands, regarding L_c, Γ_c, and X_c, agree well with experiments. Furthermore, the calculated conduction-band mass at the Γ

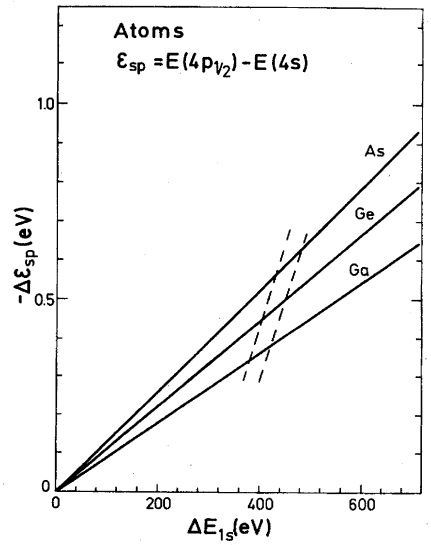

FIG. 2. Atomic calculations including extra potentials of the type given by Eq. (1). The figure shows the shift in the $4s$-$4p_{1/2}$ separation as a function of the upshift ("artificial Darwin shift") of the $1s$ level as calculated self-consistently for various choices of r_0 and V_0 in $V_w(r)$ [Eq. (1)]. The values between the dashed lines correspond to parameters optimizing the conduction bands of Ge and GaAs.

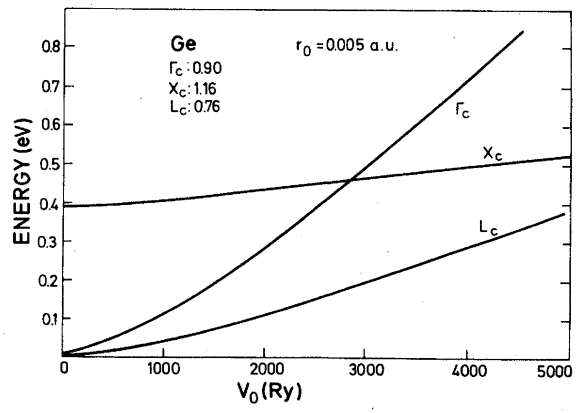

FIG. 3. Energies of conduction-band edges, measured from the valence-band top at Γ, in Ge, derived from self-consistent band calculations with extra potential [Eq. (1)] on the Ge site as a function of V_0 (r_0 fixed). No adjusting potentials are added in the "empty spheres." The figure illustrates that parameters that produce a good adjustment at Γ, in this case, do not simultaneously shift the X_c and L_c levels sufficiently. The gaps obtained in Ref. 1 are listed in the figure.

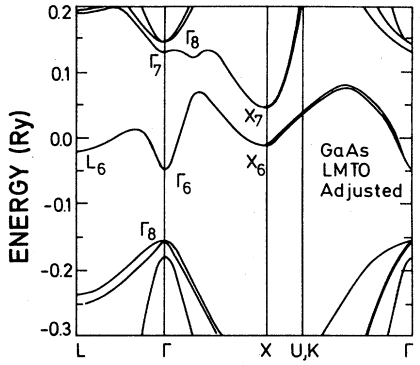

FIG. 4. Adjusted equilibrium band structure of GaAs in the gap regime. This represents our best conduction-band calculation and includes adjusting potentials. The parameters V_0 and r_0 used here are for Ga and As, V_0 and $r_0=320$ Ry and 0.015 a.u., respectively; E_1, 100 Ry and 0.4 a.u.; E_2, 250 Ry and 0.54 a.u. Furthermore, the calculation producing the self-consistent potential used here differs from that of Fig. 1 by applying only one valence-band panel. The Ga $3d$ states are treated as renormalized frozen-core states. The Ga and As spheres are larger than the "empty spheres" $S_{\mathrm{Ga}}=S_{\mathrm{As}}=3.0000$ a.u., and $S_{E_1}=S_{E_2}=2.110\,106$ a.u.

minimum is $0.068m_0$, in good agreement with experiment. The unadjusted band model gives $0.012m_0$, a value which is far too low.

The zinc-blende structure does not have the inversion symmetry of, for example, the diamond lattice. This means that Kramers degeneracy, in general, is lifted by spin-orbit coupling. This splitting of the lowest conduction band (in the [110] direction) was studied in some detail in a recent work,[16] and it was shown that, for $\vec{k}$ close to Γ, only the adjusted band structure yielded a splitting in agreement with experimental data.

It is concluded that it is possible, by adding extra potentials of the type of Eq. (1) at the atomic sites, and also at the empty-sphere sites, to adjust globally the conduction bands of predominantly s-like character. The parameters have been selected such that the bands agree well with experiments at the equilibrium volume. In the following we shall discuss volume and pressure variations of the lowest conduction band in GaAs. Such quantities derived from adjusted bands are always calculated with the same set of parameters as used to provide adjustment of the gaps at the equilibrium volume, i.e., no further (volume-dependent) adjustment is made. It is a major advantage of the corrections in terms of the very-short-range potentials [Eq. (1)] that such pressure-dependent readjustments can be avoided. Furthermore, the simple r dependence of the potentials makes their inclusion in the self-consistent local-density band calculations straightforward.

III. HYDROSTATIC DEFORMATION

Pressure coefficients of the band gaps in semiconductors have recently been calculated by Chang *et al.*[17] from first-principles pseudopotential theory. They[17] found good agreement with experiment, although the band gaps themselves are too small. Simultaneously, the ground-state properties, equilibrium volume, and bulk modulus are accurately[17] described. The calculations of Ref. 17, however, excluded (for GaAs) the relativistic effects. As mentioned before, the local-density errors in the gaps are considerably larger when these are considered, and we have therefore calculated pressure coefficients in our scheme.

The relativistic corrections do not influence the ground-state properties significantly.[5] The pressure-volume relation calculated in the present relativistic scheme (band calculations as shown in Fig. 1) is shown in Fig. 6. The calculated equilibrium volume (which corresponds to the average atomic-sphere radius $S_{\mathrm{theor}}=2.629$ a.u.) differs by only 0.15% from the experimental volume, which corresponds to $S=S_{\mathrm{expt}}=2.6303$ a.u. The bulk

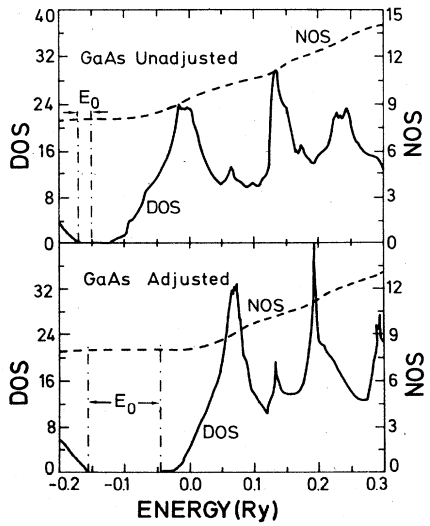

FIG. 5. GaAs conduction-band density-of-states (DOS) and number-of-states (NOS) functions for the unadjusted and adjusted band structures.

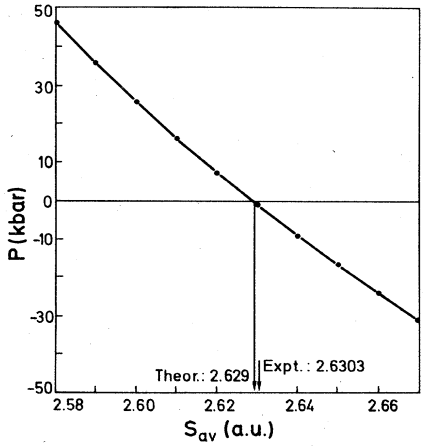

FIG. 6. Pressure P as a function of atomic-sphere radius S, calculated by means of the relativistic LMTO method including "empty spheres" and with two panels in the occupied-band regime (as in Fig. 1). No "extra potentials" added.

modulus is calculated to be 728 kbar, which is 1.5% smaller than the room-temperature value (739 kbar) and 6.5% smaller than the low-temperature value ($\sim$770 kbar). The calculated pressure dependence of the bulk modulus is shown in Fig. 7. B varies almost linearly with pressure in the range considered here, and the slope $dB/dP=4.4$ agrees well with experiments.[3]

The band gap in GaAs at normal pressure is the direct band gap E_0 at Γ. E_0 increases with pressure, whereas the conduction-band edge at X (X_6^c) decreases, and for sufficiently large pressures X_6^c is below E_0, and the gap becomes indirect. Experimental values for the pressure P_0 at which this conduction-band inversion occurs are 35 kbar (Ref. 18) and 30 kbar (Ref. 19). The nonrelativistic calculation of Ref. 17 yielded $P_0=31$ kbar, in agreement with these results. From our calculations, however, where E_0 is particularly small in the LD model, we find $P_0=73$ kbar. Only when the adjustment of the conduction band as described in Sec. II is introduced can a reasonable value be obtained. Figure 8 shows E_0 and X_6^c versus (theoretical) pressure for the adjusted bands. The inversion pressure calculated here is 30.5 kbar, i.e., in good agreement with Refs. 17–19. The calculated curve showing (Fig. 8) the variation of E_0 with pressure deviates markedly from linearity. This reflects mainly the equation of state. For volume changes up to $\sim\pm6\%$, E_0 varies essentially linearly with V (Fig. 9). We find (Fig. 9) $dE_0/d\ln V=-8.75$ eV, and from the calculated pressures we have, for the coefficient for first-order pressure dependence, $dE_0/dP=12.02$ eV/Mbar. If we use the unadjusted bands, we obtain $dE_0/dP=8.5$ eV/Mbar, which is too low when compared to experiments[18,20] (12.6 and 11.3 eV/Mbar). To second order in pressure, we write

$$E_0=E_0^0+\alpha P+\beta P^2\,, \tag{2}$$

where E_0^0 is the gap E_0 at normal pressure. Assuming the linear variation of E_0 with volume, we have

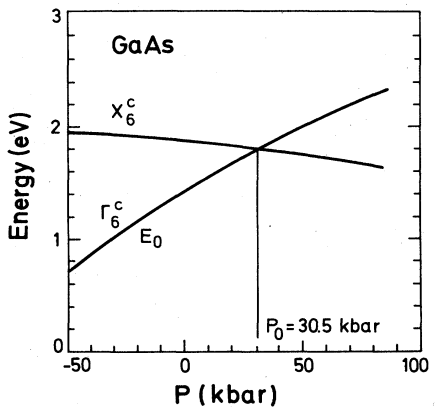

FIG. 8. Conduction-band edges at X and Γ as functions of (theoretical) pressure. The gaps are calculated from the adjusted band structure [parameters V_0 and r_0 determined at the experimental equilibrium volume (Fig. 4)] for varying volume (self-consistent at each volume).

$$\alpha=-\frac{1}{B_0}\frac{dE_0}{d\ln V}\bigg|_{P=0}\,,\quad \beta=\frac{1}{2}\frac{1}{B_0^2}\frac{dE_0}{d\ln V}\frac{dB}{dP}\,, \tag{3}$$

and with the presently calculated values of the bulk modulus at $P=0$ and dB/dP we have $\alpha=12.02$ eV/Mbar and $\beta=-36.3$ eV/Mbar^2. The room-temperature value deduced from experiments by Welber *et al.*,[18] $\beta=-37.7$ eV/Mbar^2, is in agreement with the present calculation. The β value found by Syassen[20] is somewhat smaller in magnitude, -18 eV/Mbar^2. We cannot, in our model, explain the observation made by Wolford *et al.*[21] that $\beta\simeq0$ at low temperatures ($T=5$ K).

The spin-orbit splitting at the top of the valence band (Δ_0) varies only slowly with volume (Fig. 10). The deformation potential $d\Delta_0/d\ln V$ is calculated to be approximately equal to -0.051 eV. In Fig. 10 the spin-orbit

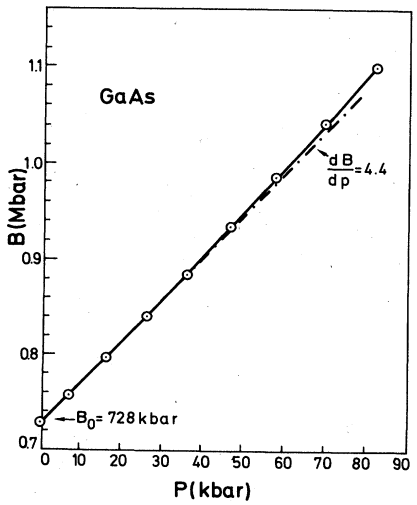

FIG. 7. Bulk modulus B versus pressure P calculated from the unadjusted bands (as in Figs. 1 and 6).

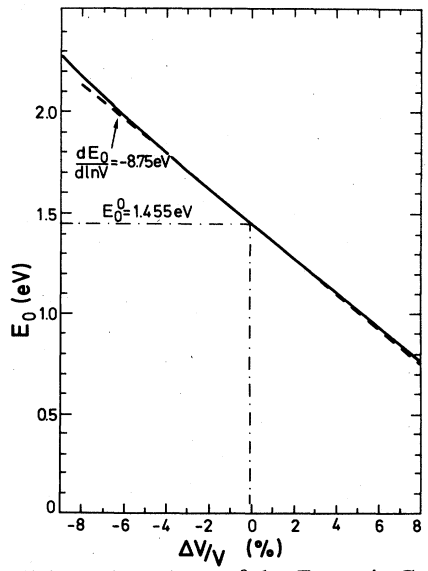

FIG. 9. Volume dependence of the E_0 gap in GaAs as calculated self-consistently with inclusion of the adjusting potentials.

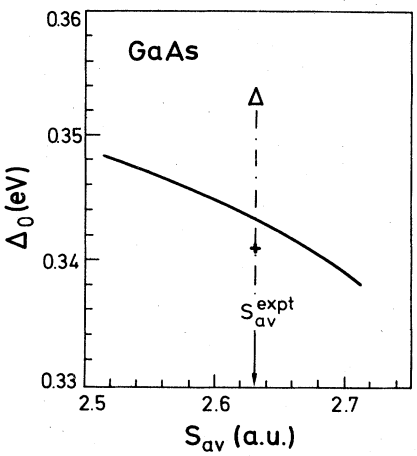

FIG. 10. Spin-orbit splitting Δ_0 at the valence-band top at Γ versus (average) atomic-sphere radius S. The triangle indicates the splitting obtained *without* extra potentials, and the plus denotes the experimental value of Δ_0 at normal volume.

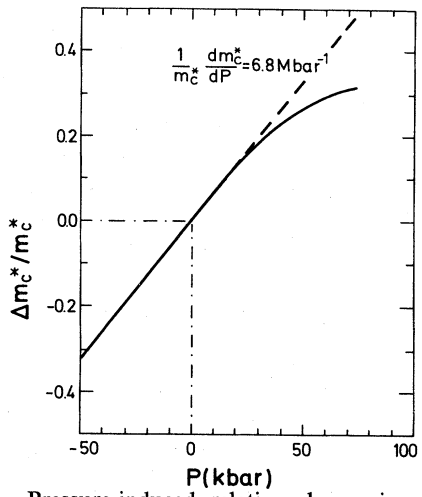

FIG. 11. Pressure-induced relative change in conduction-band mass m_c^* calculated from the adjusted self-consistent-band model.

splitting as calculated in the unadjusted band structure for $S=S_{\text{expt}}$ is indicated by a triangle (0.353 eV). The adjusted band model gives a lower value, 0.343 eV, only 0.002 eV from the observed splitting. A part of the reduction of Δ_0 when the extra potentials are added is a simple atomic effect—it is due to the change of dV/dr when $V_w(r)$ [Eq. (1)] is included. The reduction can be estimated from atomic calculations and scaling the SO splitting to the larger value at the GaAs valence-band top by means of renormalization arguments.[14,22] This yields an atomic reduction of Δ_0 of 4 meV, slightly less than half of the full band-structure shift.

"Absolute" hydrostatic deformation potentials, $a(\Gamma_{15}^v)$, $a(\Gamma_1^c)$, or when SO is included $a(\Gamma_8^v)$ and $a(\Gamma_6^c)$, for levels at the band edges at Γ, have been derived from the self-consistent LMTO calculations in the same way as was done for Si and Ge by Verges *et al.*[23] For the band model without adjusting potentials, we obtain $a(\Gamma_{15}^v)=-9.1$ eV and $a(\Gamma_1^c)=-17.0$ eV. The corresponding values obtained in Ref. 23 for Si and Ge are, for $\Gamma_{25}'^v$, -7.9 eV (Si) and -8.2 eV (Ge), and for Γ_2', -20.3 eV (Si) and -18.6 eV (Ge). Thus for GaAs we obtain very similar results. Using the adjusted band structure, and including spin-orbit coupling, we find $a(\Gamma_8^v)=-8.4$ eV and $a(\Gamma_6^c)=17.1$ eV. It was argued in Ref. 23 that, although the local-density approximation yields gaps that are too small, the "absolute hydrostatic deformation potentials" should be predicted correctly. Since our adjusted and unadjusted models give essentially the same a values, we have to some extent provided a confirmation of this assumption.

The warping of the conduction band near Γ has been studied recently by Rössler.[24] The mass, however, is isotropic. Actual numerical calculation of the conduction-band masses in the $\langle 111\rangle$, $\langle 100\rangle$, and $\langle 110\rangle$ directions differ by less than 0.7%.

A (positive) pressure increases the E_0 gap, and the conduction band near Γ becomes less steep, i.e., the mass is increased. The pressure-induced mass change as calculated (modified band model) follows from Fig. 11. At zero pressure we find $(m_c^*)^{-1}dm_c^*/dP=(6.8\pm0.3)$ Mbar^{-1}. This pressure coefficient agrees very well with the values 7.0 and 6.5 Mbar^{-1} derived from magnetophonon-effect[25] and Faraday-rotation experiments,[26] respectively. In a $\vec{k}\cdot\vec{p}$ perturbation scheme the pressure coefficient for m_c^* is

$$\frac{1}{m_c^*}\frac{\partial m_c^*}{\partial P}=\left[\frac{2(E_0+\Delta_0)}{E_0}\frac{dE_0}{dP}+\frac{E_0}{E_0+\Delta_0}\frac{d(E_0+\Delta_0)}{dP}\right]\Big/[2(E_0+\Delta_0)+E_0]\,. \tag{4}$$

Inserting here our *calculated* gaps and pressure coefficients ($E_0=1.46$ eV, $\Delta_0=0.34$ eV, $dE_0/dP=12.02$, and $d\Delta_0/dP=0.07$ eV/Mbar), Eq. (4) gives the mass-pressure coefficient of 7.9 Mbar^{-1}, i.e., slightly too large when compared to the value computed directly [(6.8 ± 0.3) Mbar^{-1}]. The *unadjusted* band model fails completely in predicting $(m_c^*)^{-1}dm_c^*/dP$; it gives 35 Mbar^{-1} [from $\vec{k}\cdot\vec{p}$ expression (4) with unadjusted band parameters.]. It is noted that the ratio between the unadjusted and adjusted pressure coefficients ($35/6.8=5.15$) is close to the ratio

$$m_c^*(\text{adjusted})/m_c^*(\text{unadjusted})=0.068/0.012=5.6\,.$$

Thus, the *absolute* pressure coefficient $dm_c^*/dP\approx0.46m_0$ Mbar^{-1} is well predicted by the unadjusted band model. This is in agreement with the observation that the two band models give essentially the same hydrostatic deformation potentials.

The splitting induced by spin-orbit coupling of the conduction band in GaAs can, to lowest order in k, be expressed[27] as

$$\Delta E=\gamma_0[k^2(k_y^2k_z^2+k_z^2k_x^2+k_x^2k_y^2)-9k_x^2k_y^2k_z^2]^{1/2}\ . \tag{5}$$

For $\vec{k}$ along [110] it follows that this lowest-order term of ΔE is proportional to k^3. The coefficient γ_0 was calculated earlier[16] from LMTO calculations as well as by treating the $\vec{k}\cdot\vec{p}$ Hamiltonian in third order. Within the latter scheme, we have[16] ($e=\hbar=m_0=1$)

$$\gamma_0=\tfrac{4}{3}PP'Q\left[\frac{\Delta_0}{E_0(E_0+\Delta_0)}\left[\frac{2}{3(E_0'-E_0+\Delta_{15})}+\frac{1}{3(E_0'-E_0)}\right]+\frac{\Delta_{15}}{(E_0'-E_0)(E_0'-E_0+\Delta_{15})}\left[\frac{2}{3E_0}+\frac{1}{3(E_0+\Delta_0)}\right]\right]. \tag{6}$$

Here, $E_0=\Gamma_6^c-\Gamma_8^v$, $E_0'=\Gamma_7^c-\Gamma_8^v$, $\Delta_{15}=\Gamma_8^c-\Gamma_7^6$, P and P' are the matrix elements of $\vec{p}$ between the Γ_1 state and $\Gamma_{15}^v,\Gamma_{15}^c$, respectively, and Q represents matrix elements between Γ_{15}^v and Γ_{15}^c (for details of notation, see Ref. 28).

The volume (and pressure) dependence of γ_0 is strongly nonlinear. This is seen in Fig. 12, where γ_0/γ_0^0 versus average atomic-sphere radius S is shown. The solid curve is calculated directly from the LMTO bands, whereas the

TABLE II. Pressure coefficients.

	Present "adjusted"	Present "unadjusted"	Other calculated	Experiments
S_{av}	2.713	2.629		2.6303 a.u.
B	810[a]	728		739 kbar[b] 770 kbar[c]
dB/dP		4.4		4.45[d]
dE_0/dP	12.02		10.6[e,f] 18.5[h,f]	12.6 eV/Mbar[g] 11.1 eV/Mbar[d] 10.6 eV/Mbar[i] 8.5 eV/Mbar[j] 11.3 eV/Mbar[j]
dE_0'/dP	0.98 eV/Mbar			
$d\Delta_0/dP$	0.07 eV/Mbar			
$d\Delta_{15}/dP$	0.11 eV/Mbar			
$(1/m_c^*)(dm_c^*/dP)$	6.8±0.3	35	7.9[k]	7.0 Mbar^{-1}[l] 6.5 Mbar^{-1}[m]
$a(\Gamma_8^v)$	−8.4	−9.1[f]	−7.3eV[h,f]	
$a(\Gamma_6^c)$	−17.1	−17.0[f]	−18.3[h,f]	(−)17.5 eV[n]
$(1/\gamma_0)(d\gamma_0/dP)$	7.6±0.7		10.0 Mbar^{-1}[k]	
P_0	30.5	73	31[e]	35 kbar[g] 30 kbar[o]
$dE(X_1^c-\Gamma_8^v)/dP$	−2.25		−2.2[e]	−2.7 eV/Mbar[o] −1.8 eV/Mbar[j]
$dE(L_1^c-\Gamma_8^v)/dP$	4.49		4.3[e]	5.5 eV/Mbar[j]

[a] At observed equilibrium volume.
[b] Reference 3, $T=300$ K.
[c] Reference 3, $T=0$ K.
[d] Reference 21.
[e] Reference 17.
[f] Without spin-orbit coupling.
[g] Reference 18.
[h] Reference 32.
[i] Reference 20.
[j] Reference 3.
[k] Present work, $\vec{k}\cdot\vec{p}$ calculation.
[l] Reference 25.
[m] Reference 26.
[n] Experiment gives magnitude, Ref. 33.
[o] Reference 19.

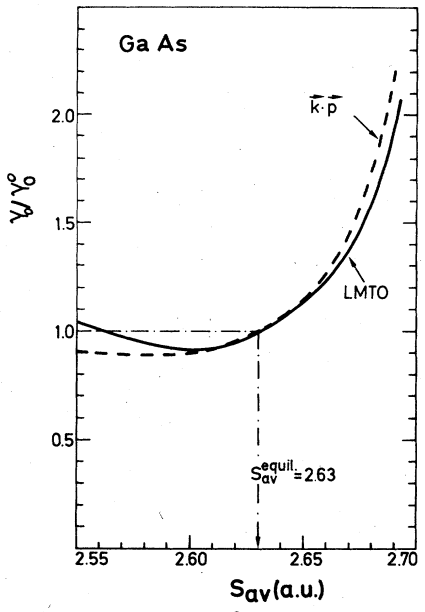

FIG. 12. Volume dependence of the spin-orbit-induced splitting of the [110] conduction band near Γ. The figure shows the coefficient γ_0 [Eq. (5)] as a function of the (average) atomic-sphere radius S. The value γ_0^0 is the equilibrium-volume value ($S_{av}=2.6303$ a.u.). The solid line represents the results calculated directly from the splitting in the LMTO bands, whereas the dashed curve is obtained from Eq. (6).

dashed curve is obtained from the $\vec{k}\cdot\vec{p}$ expression (6), keeping the matrix elements fixed and using the calculated band gaps. The value of γ_0 increases when the lattice is compressed as well as when the volume is increased, the minimum value being attained for $S\simeq 2.6$ a.u., i.e., for $P\approx 26$ kbar. The increase of γ_0 upon compression is due to the reduction of the difference between the E_0' gap and E_0 when the volume is reduced $[d(E_0'-E_0)/d\ln V = -8.75$ eV]. The coefficient for first-order volume variations at the observed equilibrium volume is, calculated from the LMTO bands,

$$\frac{1}{\gamma_0^0}\frac{d\gamma_0}{d\ln V}\simeq 5.5\pm 0.5 .$$

Differentiation of the $\vec{k}\cdot\vec{p}$ expression [Eq. (6)], assuming constant matrix elements, gives, with the LMTO gaps, 7.3.

The majority of the calculated pressure coefficients discussed in this section are summarized in Table II. Note that all conversions from volume derivatives to pressure coefficients are made by using our theoretical bulk modulus $B_0=728$ kbar. In Ref. 17 the 300-K value of 739 kbar obtained experimentally was used.

IV. UNIAXIAL STRAIN

Self-consistent LMTO calculations have been made for GaAs crystals under uniaxial strain. The purpose is to derive, from first principles, the deformation potentials for splitting of the valence-band top, and the strain dependence of the conduction-band masses. These quantities have been studied extensively experimentally,[29,30] but theoretical[30,32,34] calculations have so far mainly been made by means of empirically adjusted pseudopotential and tight-binding schemes. The strains are chosen to be strictly volume conserving for all deformations. A Bravais-lattice point, which in the undeformed lattice is at $\vec{R}$, is, under strain, moved to $\vec{R}'$, given by

$$\vec{R}'=\overleftrightarrow{E}\cdot\vec{R} , \tag{7}$$

where

$$\overleftrightarrow{E}=\begin{bmatrix} e^{-\gamma/2} & 0 & 0 \\ 0 & e^{-\gamma/2} & 0 \\ 0 & 0 & e^{\gamma} \end{bmatrix} \tag{8a}$$

for a tetragonal shear (axis, [001]). The trigonal-strain deformation matrix is given by

$$\overleftrightarrow{E}_{ij}=\begin{cases} \frac{1}{3}(e^{\gamma}+2e^{-\gamma/2}) & \text{for } i=j , \\ \frac{1}{3}(e^{\gamma}-e^{-\gamma/2}) & \text{for } i\neq j . \end{cases} \tag{8b}$$

The atomic positions in the case of a trigonal deformation are dependent on the *internal-strain* parameter[35] ζ. Choosing a coordinate system, where an As atom is at (0,0,0) and a Ga atom is at $\vec{R}_2=(a/4)(1,1,1)$ in the unstrained crystal, ζ is related to the relative sublattice displacement through

$$\vec{R}_2'=[\overleftrightarrow{E}-\zeta(\overleftrightarrow{E}-\overleftrightarrow{1})]\cdot\vec{R}_2 . \tag{9}$$

If spin-orbit coupling is omitted, the top of the valence band Γ_{15}^v is triply degenerate, not counting Kramers degeneracy. The uniaxial strains, Eqs. (8) and (9), split this into a singly (E_1) and a doubly (E_2) degenerate level. The deformation potentials b_1 and d_1 are, in the limit $\gamma\to 0$, defined[35] through

$$\delta w_0\equiv E_1-\tfrac{1}{3}(E_1+2E_2)=3b_1\gamma , \tag{10a}$$

$$\delta w_0\equiv E_1-\tfrac{1}{3}(E_1+2E_2)=\sqrt{3}d_1\gamma , \tag{10b}$$

and (10a) is for the tetragonal case, and (10b) is for the trigonal case, respectively. The spin-orbit coupling splits Γ_{15}^v into Γ_7^v and Γ_8^v. A uniaxial strain splits the upper state (Γ_8^v) into two states, separated by δw. The deformation potentials (with spin-orbit coupling) b and d are defined as in Eqs. (10), but with δw_0 replaced by δw. The effect of the spin-orbit coupling is characterized[35] by the deformation parameters b_2 and d_2:

$$b=b_1+2b_2 , \quad d=d_1+2d_2 . \tag{11}$$

As in the case of the copper halides (Ref. 36) and Si (Ref. 37) the deformation potentials derived from band calculations that are fully self-consistent for each value of γ (and ζ) are found to be identical to those calculated by the "frozen-potential" approach.[36] The trigonal-shear deformation potentials d (and d_1 and d_2) depend linearly[38–40] on the internal-strain parameter ζ:

$$d=d'-\tfrac{1}{4}d_0\zeta . \tag{12}$$

Equation (12) defines the optical deformation potential d_0. A quantity $d_{2,0}$ is defined analogously for the spin-orbit part d_2 of the trigonal deformation potential. The calculated d-versus-ζ relations, Fig. 13, clearly illustrates the linear relation, Eq. (12). The results obtained with the adjusted and unadjusted band models are very similar. Three sets of experimental data are indicated, and it follows that the value of the internal-strain parameter, which in our model would give d values in agreement with the data of Ref. 29, is $\zeta \approx 0.53$. This is the same result as obtained for Si (Ref. 37) and is close to the value 0.600 obtained by Martin[41] from a model expressing ζ in terms of elastic constants. The values of the optical-phonon deformation potential d_0, which are obtained from the slopes [see Eq. (12)] of the straight lines in Fig. 13, lie between ≈ 16.5 and 18.5 eV. These are considerably below the published value, 41 eV, derived by fitting to absolute Raman scattering intensities. The reason for this very large discrepancy is not known. Our values for d_0 are also much lower than those calculated from the empirically adjusted pseudopotentials[32,34] (36 eV).

The value which we obtain for d_2 is numerically small, $d_2 \simeq -0.05$ eV, as in the case[37] of Si. Figure 13 shows that $d_{2,0} \simeq 0$ eV.

The tetragonal-shear deformation potentials b and b_1 are both calculated to be -1.43 eV, i.e., $b_2 = 0.00$ eV. The value measured[29] by Chandrasekhar and Pollak, $b = (-1.7 \pm 0.1)$ eV, is in reasonable agreement with the present calculation.

Deformation potentials similar to those discussed for the Γ_{15}^v valence state can be introduced for the conduction-band state Γ_{15}^c (Γ_8^c). The trigonal-shear deformation potentials d_1^c and d^c are shown in Fig. 14 as functions of the internal-strain parameter. It follows that also in this case almost the same results are obtained with and without adjusting potentials. The optical deformation potentials [Eq. (12)] calculated (Fig. 14) are all $d_0^c \approx -14$ eV, and in view of the discrepancies found for d_0 this is remarkably close to result of the pseudopotential calculation,[30] giving $d_0^c = -12.0$ eV. As for the Γ_8^v state, the influence of the spin-orbit coupling is small, and d_2^c is small in magnitude and changes sign for $\zeta \approx 0.4$.

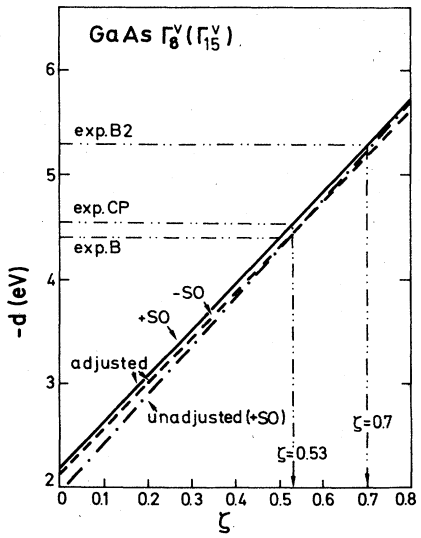

FIG. 13. Calculated trigonal-shear deformation potential d, versus internal-strain parameter ζ. The solid line is for band calculations including the extra potentials [Eq. (1)], and with spin-orbit coupling. The dashed line is calculated in the same band model, except for the omission of spin-orbit coupling. The dashed-dotted line corresponds to the unadjusted band model, with SO coupling. Experimental values of d are indicated. CP, Ref. 29; B, Ref. 40; B2, Refs. 50 and 51.

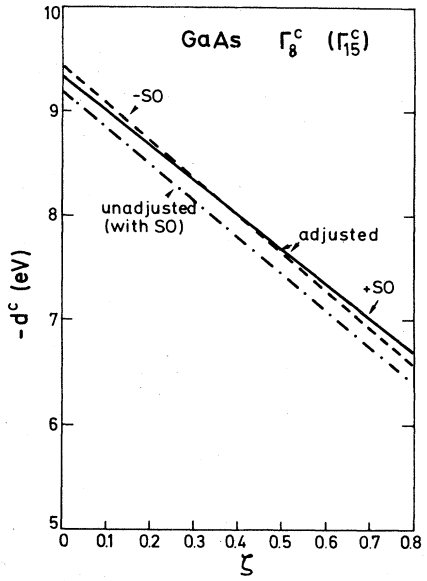

FIG. 14. Trigonal-shear deformation potential d^c for the conduction-band state Γ_8^c (Γ_{15}^c in single group notation). Solid line, adjusted band structure, with SO coupling; dashed line, without SO coupling; dashed-dotted line, unadjusted, with SO coupling.

The piezoresistance investigations by Aspnes and Cardona[30] allowed an experimental determination of the shear deformation potential $\mathscr{E}_2^L$ for the conduction-band minimum at the symmetry point L. They found[30] $\mathscr{E}_2^L = (19.6 \pm 3)$ eV. In order to check the validity of our shear calculations, particularly in view of the discrepancies for d_0, we have calculated $\mathscr{E}_2^L$ as a function of ζ. The results are shown in Fig. 15. Again, the calculations were made with and without adjusting [Eq. (1)] potentials. The results cannot be distinguished on the scale of Fig. 15. The value calculated for $\zeta = 0.53$—the internal-strain parameter for which our deformation potential d agrees with the experiment of Ref. 29 (see Fig. 14)—is $\mathscr{E}_2^L = 18.5$ eV, i.e., in good agreement with the experimental result. In evaluating this comparison, note, however, the rather large error range, ± 3 eV, on the experimental value.

The $\vec{k} \cdot \vec{p}$ perturbation-theory expression for the conduction-band mass which was used to derive Eq. (4) fails completely when applied to calculations of the shear-induced changes in the masses. It was shown[31] by Aspnes and Cardona that third-order terms had to be included in order to explain that the value of $m_{c\|}^*$ *increases* for a compression along $\langle 111 \rangle$.

The conduction-band mass is anisotropic for the crystals under uniaxial strain. This anisotropy is described in

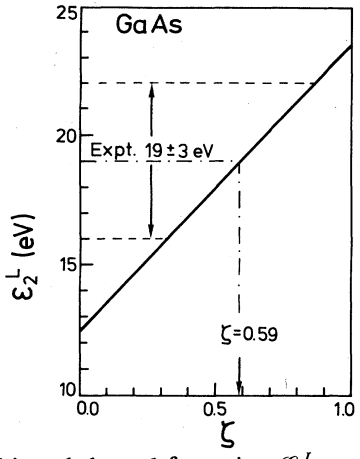

FIG. 15. Trigonal-shear deformation $\mathscr{E}_2^L$ potential for the conduction-band minimum at L, versus internal-strain parameter. Adjusted and unadjusted band models (same results).

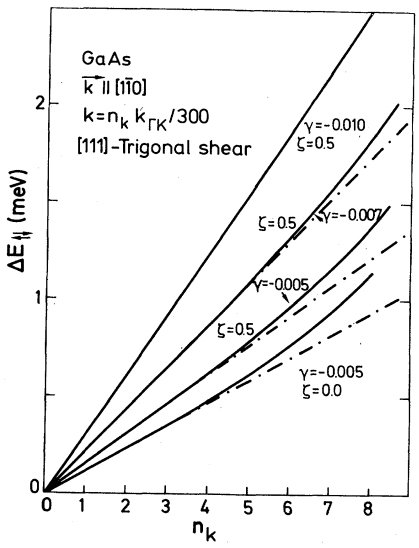

FIG. 16. Splitting of the conduction band for $\vec{k}$ along $[1\bar{1}0]$ for three different trigonal deformations, $\gamma=-0.005$, -0.007, and -0.010, where γ is the deformation parameter [see Eq. (8b)]. The internal-strain parameter is chosen to be $\zeta=0.5$ in three of the cases shown and 0.0 in one case (the lowest-lying curve). Linear contributions are shown as dashed-dotted lines.

terms of the ratio $(m_{c\parallel}^*/m_{c\perp}^*)$, where $m_{c\parallel}^*$ is the mass corresponding to the conduction-band dispersion for $\vec{k}$ in the direction of the shear axis, whereas $m_{c\perp}^*$ is the mass for $\vec{k}$ perpendicular to the shear axis. For a $\langle 111\rangle$ trigonal shear, here we calculate $m_{c\perp}^*$ from the average of the "up" and "down" bands for $\vec{k}\|[1\bar{1}0]$. The anisotropy ratio has been calculated for a series of deformations, γ ranging from -0.01 to 0.01, and for different choices of internal-strain parameter, $\zeta=0.05$ and 1.0. It appears that the mass ratio is almost independent of ζ; in all cases we find the trigonal-strain coefficient

$$\frac{d}{d\gamma}\left[\frac{m_{c\parallel}^*}{m_{c\perp}^*}\right]_{\langle 111\rangle}\simeq -8.0\ .$$

The value which we deduce from the calculations by Aspnes and Cardona[31] (shear only) is $\simeq -7.1$. Thus their perturbation calculation gives essentially the same value as the present calculation.

The trigonal-strain dependence of the mass m_c^* which we calculate corresponds to a strain coefficient

$$\left[\frac{1}{m_{c\parallel}^*}\frac{d}{d\gamma}(m_{c\parallel}^*)\right]_{\langle 111\rangle}\simeq -9\pm 3\ .$$

The relatively large error on this value reflects numerical inaccuracies in our calculations which also implies that a clear dependence on internal-strain parameter cannot be found. Again, the result which we derive from the calculations in Ref. 31, -12, agrees reasonably well with our value.

The splitting of the "up" and "down" conduction bands for $\vec{k}\|[1\bar{1}0]$ is, for small k, proportional to k^3 in the unstrained crystal. When a shear is added—as is done here in the [111] direction—additional splitting of these bands is introduced. This splitting is linear in k near Γ, as can be seen from Fig. 16. We write the strain-induced splitting as

$$\Delta E=(V_2)(\hbar k)\gamma\sqrt{2}\ . \tag{13}$$

For the trigonal shear considered here, V_2 varies linearly with the internal strain parameter ζ,

$$V_2=V_2^0+\frac{dV_2}{d\zeta}\zeta\ , \tag{14}$$

and the results of the LMTO calculations give $V_2^0=6.23\times 10^7$ cm/sec and $dV_2/d\zeta=4.2\times 10^7$ cm/sec. Thus, for $\zeta=0.53$ we find $V_2=8.46\times 10^7$ cm/sec. Recent pseudopotential calculations by Cardona *et al.*[42] for a $\langle 110\rangle$ strain gave 3.5×10^7 cm/sec, whereas Cardona and co-workers,[42] using a tight-binding scheme, found 8.7×10^7 cm/sec. Experimentally, the magnitude of V_2 has been obtained[43,44] by measuring the spin relaxation of photoexcited electrons, yielding $V_2=6\times 10^7$ cm/sec.

The changes of the conduction-band mass following a tetragonal shear (shear axis, [001]), according to the present calculations, are small compared to those found in the trigonal case. We find that a tetragonal compression only slightly affects the mass anisotropy,

$$\frac{d}{d\gamma}\left[\frac{m_{c\parallel}^*}{m_{c\perp}^*}\right]_{\langle 001\rangle}\simeq -0.9\ .$$

From Table IV of Ref. 31 we deduced the value 4.7, i.e., a value numerically larger and of the opposite sign. The tetragonal-strain coefficient for the parallel mass $m_{c\parallel}^*$ is here found to be

$$\left[\frac{1}{m_{c\parallel}^*}\frac{dm_{c\parallel}^*}{d\gamma}\right]_{\langle 001\rangle}=-3.5\ ,$$

i.e., a value having the same sign as the trigonal-shear coefficient, but only one-third of it in magnitude. The pseudopotential calculation of Ref. 31 gives a strain coefficient of 3.1, i.e., a value of the same magnitude but of

TABLE III. Uniaxial-strain parameters. (Deformation potentials are in eV.)

	Present calculation adjusted bands	Unadjusted bands	Other calculations	Experiments
d'	−2.2		2.7[b]	
d_0	16.5	18.7	36.4[b]	41[e]
$d(\zeta=0.53)$[a]	−4.54	−4.40	−2.12[b]	−4.55±0.25[f]
$d(\zeta=0.48)$	−4.18		−4.36[c]	−5.3±0.4[g]
$d_2(\zeta=0.53)$[a]	−0.05			
$d_{2,0}$	∼0.00			
b	−1.43		−2.2[b]	−1.7±0.1[f]
b_2	0.0			
$d^{c'}$	−9.2	−9.4	−7.8[b]	
$d^c(\zeta=0.53)$[a]	−8.0			
d_0^c	−13.4	−14.1	−12.0[b]	
$\mathscr{E}_2^L(\zeta=0.53)$	18.5	18.5		19.6±3[h]
$(d/d\gamma)(m_{c\|\|}^*/m_{c\perp}^*)_{\langle 111\rangle}$	−8.0		−7.1[d]	
$(d/d\gamma)(m_{c\|\|}^*/m_{c\perp}^*)_{\langle 001\rangle}$	−0.9		4.7[d]	
$(1/m_{c\|\|}^*)dm_{c\|\|}^*/d\gamma \mid_{\langle 111\rangle}$	−9±3		−12[d]	
$(1/m_{c\|\|}^*)dm_{c\|\|}^*/d\gamma \mid_{\langle 001\rangle}$	−3.5		3.1[d]	
V_2 (10^{-7})	8.5		3.5[i]	6 cm/sec
			8.7[j]	
V_1 (10^{-7})	0.2			

[a] We have chosen the value of ζ which reproduces the experimental value of d (Ref. 29).
[b] Reference 32.
[c] Reference 46.
[d] Reference 31.
[e] Reference 3.
[f] Reference 29.
[g] References 50 and 51.
[h] Reference 30.
[i] Reference 42 (pseudopotential).
[j] Reference 42 (LCAO).

opposite sign.

The tetragonal shear also influences the splitting of the "up" and "down" bands for $\vec{k}$ along [110]. To the k^3 term of the unstrained crystal is added a term linear in k, as can be seen from Fig. 16. This (for small k) linear term is written as

$$\Delta E = -(\tfrac{3}{2}\sqrt{2})(V_1)(\hbar k)\gamma \ . \tag{15}$$

We find that V_1 is much smaller in magnitude than V_2, $V_1 \simeq 0.2\times 10^7$ cm/sec, and it is therefore expected that a measurement of this quantity will be very difficult.

The calculated strain parameters obtained for the uniaxially deformed GaAs crystal are summarized in Table III.

V. CONCLUSIONS

The present self-consistent local-density calculations show that the gap in GaAs is predicted to be far too small in comparison with experiments. Since a main purpose of this examination is to calculate strain dependencies of conduction-band properties, the gaps at symmetry points have been adjusted by adding at the atomic positions, as well as in the "empty spheres," extra, sharply peaked potentials. These introduce "artificial Darwin shifts." The parameters of the adjusting potentials have been chosen at the equilibrium volume. No readjustment is made when the volume is varied.

The hydrostatic deformation potentials calculated agree, in general, with the experimental observations. This is also the case for the relative pressure-induced change in the conduction-band mass, but only for the calculation using the adjusted band model. "Absolute" deformation potentials for the valence and conduction states at Γ, X, and L are equally well described in the adjusted and the unadjusted models. The pressure-induced conduction-band inversion is predicted correctly in the adjusted band model only. The spin-orbit-induced splitting of the conduction band for $\vec{k}\,||\langle 110\rangle$ exhibits a strongly nonlinear volume dependence. It increases rapidly with expansion, and it is therefore suggested that the coefficient to the k^3 term, γ_0, at a surface can be quite different from the bulk value. The value of the coefficient γ_0 can, as shown earlier,[16] be calculated sufficiently accurately within third-order $\vec{k}\cdot\vec{p}$ perturbation theory. Using the gaps calculated for varying volume in the LMTO scheme (for the adjusted band model) in the $\vec{k}\cdot\vec{p}$ expression, we find almost the same volume dependence as calculated

directly, although the matrix elements (P,Q) are assumed to be volume independent. As follows from the $\vec{k}\cdot\vec{p}$ expression [Eq. (6)] and from direct calculations (also see Ref. 16), γ_0 depends sensitively on the gaps, and therefore very different values are obtained with the adjusted and unadjusted band models. The *unadjusted* band model used in Ref. 16 had a gap $E_0=0.65$ eV, i.e., a value larger than the calculation presented here in Fig. 1, the difference being that the earlier LMTO calculation only applied one valence-state panel and used frozen (renormalized) Ga $3d$ states, and, in addition, SO coupling was not included. With this gap[16] we found $\gamma_0=87$ eV Å^3, whereas the adjusted model gives $\gamma_0=17$ eV Å^3, which is considerably more in agreement with experiment, 22 eV Å^3 (value cited in Refs. 16 and 45). The splitting of the "up" and "down" states is only[16] strongly affected by the conduction-band adjustment for k near 0. Thus, for the calculation of precession angle[45] of the spins of photoexcited electrons, the *splitting* of the unadjusted[16] model can be used.

The uniaxial-shear deformation potentials for the valence-band top (Γ_{15}^v), conduction-band minimum at L, and the conduction-band state Γ_{15}^c agree reasonably well with experiments apart from the optical deformation potential d_0. Our calculated value is much lower ($d_0=17-19$ eV) than the cited experimental result (41 eV). Our LMTO calculations include "empty spheres" and the so-called combined correction term.[11] The state Γ_{15}^v is particularly sensitive to this correction. If we, for a given potential, omit this term, then the Γ_{15}^v level is changed (reduced) by ≈ 1 eV. It could be argued that this reflects that this state is particularly sensitive to nonspherical terms in the potential, and therefore it may not be properly described even when we include the correction term. However, the comparison in Ref. 5 between self-consistent pseudopotential calculations, which, of course, includes the effects of the nonspherical charge distribution, and the LMTO calculations using an identical prescription for construction of the potentials, showed that the two methods give the same energy eigenvalues in the case of GaAs. Furthermore, the calculation of d in Si performed by Nielsen (see Ref. 37) for the same value of ζ as used in our[37] calculation yielded almost the same result. Very recently,[46] Nielsen and Martin calculated, using first-principles pseudopotentials, d_0 for Si, and found $d_0=29.83$ eV. This is in reasonable agreement with our result[37] (22 eV), and the consistency concerning the values of ζ obtained in Refs. 47 and 37 for Si, and the above-mentioned agreement with pseudopotential calculations,[5] suggest in our opinion that nonspherical terms are sufficiently accounted for by inclusion of the empty spheres and the combined correction term.

It was found,[37] in the case of Si, that although our LMTO band-structure calculation gives quite accurate eigenvalues, the total-energy calculations are not, with the present approximations, sufficiently accurate to allow a direct, first-principles calculation of the internal-strain parameter.[48] This is in agreement with the observations of the importance of the inclusion of nonspherical charge distributions for the calculation of elastic shear moduli.[49,50] The value of ζ, which, in our calculation, produces agreement with the observed[29] deformation potential d ($=-4.55$ eV), is $\zeta=0.53$. This is the same as found for Si.[37,47] Other experiments give values of d which are larger than that of Ref. 29. For example, Balslev[51] found $d=(-5.3\pm0.4)$ eV, a value which is (cautiously) recommended by Lawaetz.[52] This value would, according to Fig. 13, correspond to $\zeta=0.7$. The L deformation potential $\mathscr{E}_2^L$ which we calculate for this value of ζ is 20 eV, and that agrees as well as the $\zeta=0.53$ value (18.5 eV) with experiment [(19±3) eV]. Thus, our comparison of calculated trigonal-shear deformation potentials to experiments does not allow us to determine ζ in GaAs more accurately than $\zeta\simeq 0.6\pm0.1$. An independent determination by comparison of the calculated variation with ζ of the coefficient V_2 for strain-induced splitting of the conduction band for $\vec{k}$ along [110] to spin-relaxation experiments does not improve this situation. With the present computational accuracy and accuracy of the experiment, the finding that theory and experiment agree within $\sim 2\times10^7$ cm/sec is quite satisfactory.

The value $\zeta=0.48$ obtained recently from first-principles pseudopotentials[46,48] differs significantly from the result obtained by Cardona *et al.*,[53] $\zeta=0.72$. Experimental determinations of the internal-strain parameter are also somewhat contradictory[53,54] for Si, in which much data exist (they range from 0.65 to 0.75, all larger than the theoretical[47] value). In view of the difficulties in determining[54] the intensity in the "forbidden" x-ray intensities, such scatter in the experimental results is not surprising. For GaAs there exists, to our knowledge, only one experimental determination[55] of ζ, $\zeta=0.764$. This value appears large compared to the calculations Refs. 51 and 52 and the present results, but is in agreement with the calculation in Ref. 53. In order to determine the value of ζ for GaAs more accurately, more detailed experimental and theoretical investigations will be needed.

ACKNOWLEDGMENTS

The author is grateful to G. B. Bachelet and M. Cardona for helpful discussions, and to M. Hanfland and K. Syassen for communicating their experimental results prior to publication. O. H. Nielsen and R. M. Martin are thanked for communicating their recent results and for allowing us to refer to them, although not yet published.

*Permanent address: Physics Lab I, Technical University, DK-2800 Lyngby, Denmark.

[1]J. R. Chelikowsky and M. L. Cohen, Phys. Rev. B **14**, 556 (1976).

[2]J. S. Blakemore, J. Appl. Phys. **53**, R123 (1982).

[3]M. Cardona and G. Harbeke, in *Landolt-Börnstein Numerical Data and Functional Relationships in Science and Technology*, New Series, edited by O. Madelung (Springer, Berlin, 1982), Vol. 17a.

[4]D. R. Hamann, Phys. Rev. Lett. **42**, 662 (1979).

[5]G. B. Bachelet and N. E. Christensen, Phys. Rev. B (to be published).

[6]Wang and Klein (Ref. 7) found good agreement between the calculated and observed conduction-band masses. We assume

that this is mainly due to their omission of relativistic effects.
[7]C. S. Wang and B. M. Klein, Phys. Rev. B **24**, 3393 (1981).
[8]D. M. Ceperley and B. J. Alder, Phys. Rev. Lett. **45**, 566 (1980).
[9]J. Perdew and A. Zunger, Phys. Rev. B **23**, 5048 (1981).
[10]A. H. MacDonald and S. H. Vosko, J. Phys. C **12**, 2977 (1979).
[11]O. K. Andersen, Phys. Rev. B **12**, 3060 (1975).
[12]T. Jarlborg and A. J. Freeman, Phys. Lett. **74A**, 349 (1979).
[13]D. Glötzel, B. Segall, and O. K. Andersen, Solid State Commun. **36**, 403 (1980).
[14]N. E. Christensen, Int. J. Quant. Chem. **25**, 233 (1984).
[15]H. V. A. M. Rompa, M. F. H. Schuurmans, and F. Williams, Phys. Rev. Lett. **52**, 675 (1984).
[16]N. E. Christensen and M. Cardona, Solid State Commun. **51**, 491 (1984).
[17]K. J. Chang, S. Froyen, and M. L. Cohen, Solid State Commun. **50**, 105 (1984).
[18]B. Welber, M. Cardona, C. K. Kim, and S. Rodriguez, Phys. Rev. B **12**, 5729 (1975).
[19]P. Y. Yu and B. Welber, Solid State Commun. **25**, 209 (1978).
[20]M. Hanfland and K. Syassen, unpublished and private communication.
[21]D. J. Wolford and J. A. Bradley, Bull. Am. Phys. Soc. **29**, 291 (1984).
[22]To first order, the energy-dependent spin-orbit parameter of an l band can be expressed as $\zeta_l(E)\simeq\zeta_{l_0}+(E-C_l)\dot{\zeta}_l$, where the energy derivative $\dot{\zeta}_l=\mu_+/\mu_-$, the ratio between the mass parameters for $j=l-1/2$ and $l+1/2$ (see Ref. 14).
[23]J. A. Verges, D. Glötzel, M. Cardona, and O. K. Andersen, Phys. Status Solidi B **113**, 519 (1982).
[24]U. Rössler, Solid State Commun. **49**, 143 (1984).
[25]G. D. Pitt, J. Lees, R. A. Hoult, and R. A. Stradling, J. Phys. C **6**, 3282 (1973).
[26]W. M. DeMeis, Technical Report HP-15, Harvard University, 1965 (unpublished).
[27]E. O. Kane, J. Phys. Chem. Solids **1**, 249 (1957).
[28]M. Cardona, J. Phys. Chem. Solids **24**, 1543 (1963).
[29]M. Chandrasekhar and F. H. Pollak, Phys. Rev. B **15**, 2127 (1977).
[30]D. E. Aspnes and M. Cardona, Phys. Rev. B **17**, 741 (1978).
[31]D. E. Aspnes and M. Cardona, Phys. Rev. B **17**, 726 (1978).
[32]A. Blacha, H. Presting, and M. Cardona, Phys. Status Solidi B (to be published).
[33]P. Melz, J. Chem. Solids **32**, 209 (1971).
[34]W. Pötz and P. Vogel, Phys. Rev. B **24**, 2025 (1981).
[35]L. Kleinmann, Phys. Rev. **128**, 2614 (1962). For definitions of deformation potentials, also see C. Hensel and K. Suzuki, Phys. Rev. B **9**, 4219 (1974).
[36]N. E. Christensen, Phys. Status Solidi B **123**, 281 (1984).
[37]N. E. Christensen, Solid State Commun. **50**, 177 (1984).
[38]W. Richter, in *Solid State Physics,* edited by G. Höhler (Springer, Heidelberg, 1976).
[39]J. L. Ivey, Phys. Rev. B **9**, 4231 (1974).
[40]I. Balslev, Solid State Commun. **5**, 315 (1967).
[41]R. M. Martin, Phys. Rev. B **1**, 4005 (1970).
[42]M. Cardona, V. A. Maruschak, and A. N. Titkov, Solid State Commun. **50**, 701 (1984).
[43]M. I. Dyakonov, V. I. Perel, M. I. Stepanova, V. A. Maruschak, and A. N. Titkov, Izv. Akad. Nauk USSR, Ser. Phys. **47**, 231 (1983).
[44]V. A. Maruschak and A. N. Titkov, Fiz. Tverd. Tela (Leningrad) (to be published) [Sov. Phys.—Solid State (to be published)].
[45]H. Reichert, S. F. Alvarado, A. N. Titkov, and V. I. Safarov, Phys. Rev. Lett. **52**, 2297 (1984).
[46]O. H. Nielsen and R. M. Martin (unpublished); O. H. Nielsen (private communication).
[47]O. H. Nielsen and R. M. Martin, Phys. Rev. Lett. **50**, 697 (1983).
[48]During the preparation of this manuscript, we were informed that Nielsen and Martin calculated ζ for GaAs in the same way as for Si (Ref. 47). They found $\zeta=0.48\pm0.02$ (Ref. 46). Furthermore, they calculated d for this value of ζ, and the value, -4.36 eV, agrees well with ours, -4.18 eV (Table III).
[49]N. E. Christensen, Solid State Commun. **49**, 701 (1983).
[50]N. E. Christensen, Phys. Rev. B **29**, 5547 (1984).
[51]I. Balslev, Phys. Rev. **177**, 1173 (1969).
[52]P. Lawaetz, thesis, Technical University of Denmark, 1978.
[53]M. Cardona, K. Kunc, and R. M. Martin, Solid State Commun. **44**, 1205 (1982).
[54]For a review, see C. S. G. Cousins, J. Phys. C **15**, 1857 (1982).
[55]C. N. Koumelis, G. E. Zardas, C. A. Londos, and D. K. Leventuri, Acta Crystallogr. Sect. A **32**, 84 (1975).